

**MATHEMATICAL ENGINEERING
TECHNICAL REPORTS**

**Phase diagrams and correlation inequalities of
a three-state stochastic epidemic model on the
square lattice**

Kazumichi Ohtsuka, Norio Konno, Naoki Masuda and
Kazuyuki Aihara

METR2005-33

October 2005

DEPARTMENT OF MATHEMATICAL INFORMATICS
GRADUATE SCHOOL OF INFORMATION SCIENCE AND TECHNOLOGY
THE UNIVERSITY OF TOKYO
BUNKYO-KU, TOKYO 113-8656, JAPAN

WWW page: <http://www.i.u-tokyo.ac.jp/mi/mi-e.htm>

The METR technical reports are published as a means to ensure timely dissemination of scholarly and technical work on a non-commercial basis. Copyright and all rights therein are maintained by the authors or by other copyright holders, notwithstanding that they have offered their works here electronically. It is understood that all persons copying this information will adhere to the terms and constraints invoked by each author's copyright. These works may not be reposted without the explicit permission of the copyright holder.

Phase diagrams and correlation inequalities of a three-state stochastic epidemic model on the square lattice

Kazumichi Ohtsuka^{1,2}, Norio Konno³, Naoki Masuda^{1,4} and Kazuyuki Aihara^{1,5}

¹Aihara Complexity Modelling Project, ERATO, JST,
3-23-5, Uehara, Shibuya, Tokyo 151-0064, Japan

²Research Center for Advanced Science and Technology,
The University of Tokyo, 4-6-1, Komaba, Meguro, Tokyo 153-8505, Japan
E-mail: ohtsuka@fin.rcast.u-tokyo.ac.jp

³Faculty of Engineering, Yokohama National University,
79-5, Tokiwadai, Hodogaya, Yokohama 240-8501, Japan
E-mail: norio@mathlab.sci.ynu.ac.jp

⁴Laboratory for Mathematical Neuroscience, RIKEN Brain Science Institute,
2-1, Hirosawa, Wako, Saitama 351-0198, Japan
E-mail: masuda@brain.riken.jp

⁵Institute of Industrial Science, The University of Tokyo,
4-6-1, Komaba, Meguro, Tokyo 153-8505, Japan
E-mail: aihara@sat.t.u-tokyo.ac.jp

October 27th, 2005

Abstract

We study a three-state stochastic particle system on the square lattice, which extends the contact process. The phase diagram is analyzed by the mean-field approximation, the pair approximation, and numerics. The pair approximation turns out to be better than the meanfield ansatz. We also show that the Harris-FKG type correlation inequalities approximately hold in the present model.

1 Introduction

Modeling spreads of infectious diseases or multispecies ecological processes potentially serve to prevent epidemic outbreaks. Both nonspatial/spatial deterministic models [1, 2] and spatial stochastic models, which are mainly spatial [6, 3, 5, 4, 7], are main tools to address these issues. Among stochastic models, the contact process [5, 4], which is a two-state model and corresponds to the stochastic spatial version of the SIS model [3], is known to show various phenomena relevant to real epidemics, such as phase transitions and clustering of infectious patients. Adding the number of states or species is a natural extension of the model. For instance, the paper-scissors-stone (PSS) model and the susceptible-infected-recovered-susceptible (SIRS) model [8] have been investigated as non-hierarchical competitive community systems.

We investigate a stochastic epidemic model on the square lattice called the spatial stochastic epidemic (SSE) model. This model has three states. The model is also of physical interest because of its yet undermined phase diagram [9]. Whether coexistence of the three states really occur is not known [10, 11]. We analyze this model by the meanfield approximation (MFA), the pair approximation (PA), and Monte Carlo (MC) simulations, along a similar line with [2, 8, 9, 12, 13, 14]. Our particular focus is on the phase diagram and correlation inequalities by the pair approximation and numerical simulations.

In Sec. II, we define the SSE model and derive the dynamical equations for order parameters. In Sec. III, phase diagrams are derived from the MFA, the PA, and MC simulations. Section IV is devoted to analysis of the correlation inequalities.

2 Model

The SSE model is a continuous-time Markov process with a state space $\{0, 1, 2\}^{\mathbf{Z}^2}$, where \mathbf{Z}^2 indicates the square lattice. States 0, 1, and 2 correspond to empty, healthy, and infected, respectively. As schematically shown in Figs. 1(a) and 1(b), birth ($0 \rightarrow 1$) occurs at a rate proportional to the number of healthy sites (state 1) in the neighborhood of an empty site (state 0). We denote this rate by λn_1 , where n_i ($i = 1, 2$) is the number of neighbors in state i . Similarly, infection ($1 \rightarrow 2$) occurs at a rate μn_2 . Death from 1 to 0 and from 2 to 0 occurs at rates δ and 1, respectively. In contrast to birth or infection events, the death events occur independently of the states of the neighborhood sites. We define

$$\rho(i) \equiv \text{P}[\eta(x, y) = i], \quad (1)$$

$$\rho(ij) \equiv \text{P}[\eta(x, y) = i, \eta(x + x', y + y') = j], \quad (2)$$

$$\rho(ijk) \equiv \text{P}[\eta(x+x', y+y') = i, \eta(x, y) = j, \eta(x+1, y) = k], \quad (3)$$

where $\eta(x, y)$ is the state of $(x, y) \in \mathbf{Z}^2$, $|x'| + |y'| = 1$, and P denotes the probability. In Eq. (3), we assume that the three sites do not overlap and ignore the difference between two events $\{\eta_i(x-1, y), \eta_j(x, y), \eta_k(x+1, y)\}$ and $\{\eta_i(x, y+1), \eta_j(x, y), \eta_k(x+1, y)\}$. The dynamics of $\rho(i)$ and $\rho(ij)$ are given as follows:

$$\frac{d\rho(0)}{dt} = -4\lambda\rho(01) + \delta\rho(1) + \rho(2), \quad (4)$$

$$\frac{d\rho(1)}{dt} = 4\lambda\rho(01) - 4\mu\rho(12) - \delta\rho(1), \quad (5)$$

$$\frac{d\rho(2)}{dt} = 4\mu\rho(12) - \rho(2), \quad (6)$$

$$\frac{d\rho(00)}{dt} = -6\lambda\rho(001) + 2\delta\rho(01) + 2\rho(02), \quad (7)$$

$$\frac{d\rho(11)}{dt} = 6\lambda\rho(101) + 2\lambda\rho(01) - 6\mu\rho(112) - 2\delta\rho(11), \quad (8)$$

$$\frac{d\rho(22)}{dt} = 6\mu\rho(212) + 2\mu\rho(12) - 2\rho(22), \quad (9)$$

$$\frac{d\rho(01)}{dt} = 3\lambda\{\rho(001) - \rho(101)\} - 3\mu\rho(012) - (\lambda + \delta)\rho(01) + \delta\rho(11) + \rho(120), \quad (10)$$

$$\frac{d\rho(02)}{dt} = -3\lambda\rho(102) + 3\mu\rho(012) - \rho(02) + \delta\rho(12) + \rho(22), \quad (11)$$

$$\frac{d\rho(12)}{dt} = 3\lambda\rho(102) + 3\mu\{\rho(112) - \rho(212)\} - (\mu + \delta + 1)\rho(12). \quad (12)$$

The relations between the singlet, doublet, and triplet densities evaluated at the steady state define the correlation identities.

3 Phase diagrams

3.1 Mean field approximation

By solving the steady state of Eqs. (4)–(6) with $\rho(ij) = \rho(i)\rho(j)$, we obtain $\rho_{\text{MF}}(0) = (4\mu - 1 + \delta)/4(\mu + \lambda)$, $\rho_{\text{MF}}(1) = 1/4\mu$, and $\rho_{\text{MF}}(2) = (4\mu\lambda - \lambda - \delta\mu)/4\mu(\mu + \lambda)$. In the case when $\rho(2)$ is extinct, we set $\rho(2) = 0$ and derive $\rho_{\text{MF}}(0) = \delta/(4\lambda)$ and $\rho_{\text{MF}}(1) = (4\lambda - \delta)/(4\lambda)$. These solutions agree with the MFA solution of the CP. Then, the phases S_{01} (coexistence of 0 and 1) and S_{012} (coexistence of 0, 1, and 2) are divided by $\mu = \lambda/(4\lambda - \delta)$. When $\delta = 0$, S_1 (state 1 only) naturally appears instead of S_{01} and S_0 . When $\delta > 0$, $\lambda = \delta/4$ divides S_0 (state 0 only) and S_{01} ; this relation is independent of μ . The phase diagrams for $\delta = 0$ and $\delta = 1$ are respectively shown in Figs. 1(a) and (b), with the critical lines indicated by solid lines. Two critical lines in Fig. 1(b) approach each other as μ tends large.

3.2 Pair approximation

We next apply the PA, which takes into account two-site correlations. With the ansatz $\rho(ijk) = \rho(ij)\rho(jk)/\rho(j)$, Eqs. (7)–(12) at the steady state become:

$$0 = -6\lambda \frac{\rho(00)\rho(01)}{1 - \rho(1) - \rho(2)} + 2\delta\rho(01) + 2\rho(02), \quad (13)$$

$$0 = 6\lambda \frac{\rho(10)^2}{1 - \rho(1) - \rho(2)} + 2\lambda\rho(01) - 6\mu \frac{\rho(11)\rho(12)}{\rho(1)} - 2\delta\rho(11), \quad (14)$$

$$0 = 6\mu \frac{\rho(12)^2}{\rho(1)} + 2\mu\rho(12) - 2\rho(22), \quad (15)$$

$$0 = 3\lambda \frac{\rho(00)\rho(01) - \rho(01)^2}{1 - \rho(1) - \rho(2)} - 3\mu \frac{\rho(01)\rho(12)}{\rho(1)} + \delta\rho(11) - (\lambda + \delta)\rho(01) + \rho(12), \quad (16)$$

$$0 = -3\lambda \frac{\rho(01)\rho(02)}{1 - \rho(1) - \rho(2)} + 3\mu \frac{\rho(01)\rho(12)}{\rho(1)} + \delta\rho(12) + \rho(22) - \rho(02), \quad (17)$$

$$0 = 3\lambda \frac{\rho(01)\rho(02)}{1 - \rho(1) - \rho(2)} + 3\mu \frac{\rho(11)\rho(12) - \rho(12)^2}{\rho(1)} - (\mu + \delta + 1)\rho(12). \quad (18)$$

From Eqs. (4) and (6), we obtain

$$\rho(01) = \frac{\delta\rho(1) + \rho(2)}{4\lambda}, \quad (19)$$

$$\rho(12) = \frac{\rho(2)}{4\mu}, \quad (20)$$

respectively. Note that

$$\rho(i) = \rho(i0) + \rho(i1) + \rho(i2), \quad (i = 0, 1, 2). \quad (21)$$

Substituting Eqs. (19)–(21) into Eqs. (16)–(18) results in

$$\begin{aligned} \frac{\rho(02)}{1 - \rho(1) - \rho(2)} &= -\frac{\delta\rho(1) + \rho(2)}{2\lambda(1 - \rho(1) - \rho(2))} \\ &\quad + \frac{8\delta(3\lambda - \delta)\rho(1) + \left\{8\lambda - 11\delta + \frac{4\lambda(1-\delta)}{\mu}\right\}\rho(2) - \frac{3\rho(2)^2}{\rho(1)}}{12\lambda(\delta\rho(1) + \rho(2))}, \end{aligned} \quad (22)$$

$$\frac{\rho(02)}{1 - \rho(1) - \rho(2)} = \frac{\left(\frac{3\delta+16\lambda}{4\lambda} + \frac{\delta-1}{\mu}\right)\rho(1) + \frac{3}{4\lambda}\rho(2)}{8 + (3\delta - 8)\rho(1) - 5\rho(2)} \frac{\rho(2)}{\rho(1)}, \quad (23)$$

$$\frac{\rho(02)}{1 - \rho(1) - \rho(2)} = \frac{\left(\frac{1}{4\lambda} + \frac{1}{2\mu}\right)\rho(2) + \left(\frac{\delta}{4\lambda} - \frac{2\mu-\delta-1}{3\mu}\right)\rho(1)}{\delta\rho(1) + \rho(2)} \frac{\rho(2)}{\rho(1)}. \quad (24)$$

Substituting $\rho(2) = 0$ into Eq. (22), we have for the S_{01} phase

$$\rho(1) = \frac{12\lambda - 4\delta}{12\lambda - \delta}. \quad (25)$$

Then assuming $\rho(2) = 0$ in Eqs. (23) and (24), and substituting Eq. (25) into these equations, we have

$$\mu = \frac{12\lambda^2 + 4\lambda}{36\lambda^2 + (8 - 12\delta)\lambda - 3\delta}. \quad (26)$$

This line divides the S_{01} and S_{012} phases, which extends the result for $\delta = 1$ [12].

To solve for steady densities quantitatively, let $Q_i = \rho(i)/\rho(2)$ ($i = 0, 1, 2$). By using Eqs. (19)-(21), Eqs. (13)-(15) are transformed into

$$\frac{\rho(02)}{\rho(2)} = \frac{\left(1 - \frac{\delta}{3\lambda}\right)Q_0 - \frac{1}{4\lambda}(1 + \delta Q_1)}{3(1 + \delta Q_1) + 4Q_0} \left\{3(1 + \delta Q_1)\right\}, \quad (27)$$

$$0 = \frac{(1 + \delta Q_1)^2}{\lambda Q_0} - \left(\frac{8}{3} - \frac{\delta}{\lambda}\right) + \left(\frac{1}{Q_1} + \frac{4\delta}{3}\right) \left(\frac{1}{\lambda} + \frac{1}{\mu}\right) - 4\delta \left(1 - \frac{\delta}{3\lambda}\right) Q_1, \quad (28)$$

$$\frac{\rho(02)}{\rho(2)} = -\frac{3}{16\mu Q_1} + \frac{1}{4} \left(3 - \frac{1}{\mu}\right). \quad (29)$$

Substituting Eq. (29) into Eq. (27),

$$Q_0 = \frac{\left(3\mu\delta^2\right)Q_1^2 + \left(9\lambda\mu\delta + 6\mu\delta - 3\lambda\delta\right)Q_1 + \left(9\lambda\mu + 3\mu - 3\lambda - \frac{9\lambda\delta}{4}\right) - \frac{9\lambda}{4} \frac{1}{Q_1}}{\left[\left(12\lambda\mu\delta - 4\mu\delta^2\right)Q_1 + \left(4\lambda - 4\mu\delta\right) + 3\lambda \frac{1}{Q_1}\right]}. \quad (30)$$

By using Eqs. (28) and (30), we have

$$\begin{aligned} 0 = & 4\delta^2 \left\{9\lambda\mu - 3\lambda + 2\mu - 1 - 3\mu\delta \left(1 + \frac{1}{4\lambda}\right)\right\} Q_1^4 \\ & + \delta \left\{60\lambda\mu - 20\lambda + 16\mu - 8 - \delta \left(21\lambda + 33\mu - 3\delta - \frac{4\lambda}{\mu} + \frac{9\mu}{\lambda} + 3\right)\right\} Q_1^3 \\ & + \left\{24\lambda\mu - 8\lambda + 8\mu - 4 - \delta \left(36\lambda + 30\mu + 6 - \frac{7\lambda}{\mu} + \frac{9\mu}{\lambda} - \frac{33\delta}{4} - \frac{3\lambda\delta}{\mu}\right)\right\} Q_1^2 \\ & - 3 \left\{5\lambda + 3\mu - \frac{\lambda}{\mu} + \frac{\mu}{\lambda} + 1 - \frac{\delta}{4} \left(10 + \frac{7\lambda}{\mu}\right)\right\} Q_1 + \frac{9}{4} \left(1 + \frac{\lambda}{\mu}\right). \end{aligned} \quad (31)$$

Steady densities $\rho(i) = Q_i/(1 + Q_0 + Q_1)$ are numerically given by solving Eqs. (27)-(31). Since Eq. (31) is the fourth order equation, we have four

solutions from this equation, but obtain only one solution of Q_1 satisfying both positive real number $\rho(i)$ and $0 < \rho(i) < 1$. Dashed lines in Fig. 1 are the critical lines obtained by the PA. When $\delta = 0$, we can solve them analytically [14]. ***When $\delta > 0$, the parameter region of S_0 becomes $\lambda < \delta/3$, which is larger than the MFA counterpart. As shown in Fig. 1(b), the two critical lines never intersect as $\mu \rightarrow \infty$, which contrasts to the MFA prediction. In S_{01} , the PA solution of Eqs. (13)-(20) with $\rho(2) = 0$ reads:

$$\begin{aligned} \rho(0) &= \frac{3\delta}{12\lambda - \delta}, & \rho(1) &= \frac{12\lambda - 4\delta}{12\lambda - \delta}, & \rho(00) &= \frac{\delta^2}{\lambda(12\lambda - \delta)}, \\ \rho(01) &= \frac{3\lambda - \delta}{12\lambda - \delta}, & \rho(11) &= \frac{(4\lambda - \delta)(3\lambda - \delta)}{\lambda(12\lambda - \delta)}. \end{aligned}$$

3.3 Monte Carlo simulation

To perform simulations, we initially let each site randomly have either state 0, 1, or 2 with probability 1/3. The simulation time step is the smaller of $\Delta t = (1.0 \times 10^{-3})/\lambda$ or $(1.0 \times 10^{-3})/\mu$, and each trial lasted until 2000 unit time or when extinction is reached.

Solid circles in Fig. 1 represent numerically obtained critical lines on the 100×100 lattice with periodic boundary conditions. When $\delta = 1$, the critical line between S_0 and S_{01} naturally contains $(\lambda_c, \mu) = (0.41, 0)$, where λ_c is the critical infection rate of the contact process [5, 4].

Generally, the critical lines obtained by the PA is more accurate than the those obtained by the MFA. When $\delta = 0$, the critical line between S_1 and S_{012} depends on μ , as for the PA (Fig. 1(a)). More importantly, the two critical lines do not approach each other as $\mu \rightarrow \infty$. For $\delta = 0$ and 1, values of stationary $\rho(i)$ obtained by the three methods are compared in Figs. 2 and 3. The PA better approximates numerically obtained $\rho(i)$. We also find paradoxical effects in Fig. 2(b), namely, increased λ lowers $\rho(1)$, as is known for $\delta = 0$ [14, 15] (also see our Fig. 2(a)) and the paper-scissors-stone game [13, 16]. Similarly, $\rho(2)$ does not increase monotonically in μ (Fig. 3). These results suggest that the PA is better than the MFA.

4 Correlation inequalities

In the case of the contact process, the Harris-FKG inequality (see Lemmas 3.3.4 (1) and 3.3.5 (1) of [17]) reads $\rho(ii)/\rho(i)^2 \geq 1$ ($i = 0, 1$). Remark that the inequality is also called positive correlations that are satisfied in a wide class of two-state monotone (or attractive) interacting particle systems (for more details, see pp.77-83 in [4]). However it is not known rigorously whether or not the same type of correlation inequalities, that is,

$$\frac{\rho(ii)}{\rho(i)^2} \geq 1, \quad (i = 0, 1, 2) \quad (32)$$

hold for the present three-state model.

Figure 6 shows that the results by the PA and MC simulations roughly satisfy Eq. (32). In addition, $\rho(ii)/\rho(i)^2$ when $\delta = 0$ is always larger than when $\delta = 1$ except for $\rho(22)/\rho(2)^2$. This is because $\delta > 0$ enhances mixing of the three states. Only the case $\rho(22)/\rho(2)^2$ is opposite to our intuition. A similar property is observed for the PSS model with perturbation effects [13].

5 Conclusion

We have investigated a three-state stochastic epidemic model on the square lattice. The phase transitions are analyzed by the MFA, the PA and MC simulations. The critical lines obtained by the PA and MC simulations generalize the results in [9, 12] to arbitrary δ . Correlation inequalities also hold approximately.

References

- [1] W. H. Hammer, *Lancet* **1**, 733 (1906).
- [2] R. M. Andersson and M. May, *Infectious Diseases of Humans: Dynamics and Control* (Oxford University Press, Oxford, 1992).
- [3] H. Andersson and T. Britton, *Stochastic Epidemic Models and Their Statistical Analysis* (Springer-Verlag, New York, 2000).
- [4] T. M. Liggett, *Interacting Particle Systems* (Springer-Verlag, New York, 1985).
- [5] J. Marro and R. Dickman, *Nonequilibrium Phase Transition in Lattice Models* (Cambridge University Press, Cambridge, 1999).
- [6] M. S. Bartlett, *J. R. Stat. Soc. B* **11**, 211 (1949)
- [7] N. Masuda, N. Konno and K. Aihara, *Phys. Rev. E* **69**, 031917 (2004).
- [8] J. Joo and J. L. Lebowitz, *Phys. Rev. E*, **70** 036114 (2004)
- [9] K. Sato and N. Konno, *J. Phys. Soc. Jpn.* **64**, 1866 (1995).
- [10] R. B. Schinazi, N. Konno and H. Tanemura, *Markov Processes Relat. Fields* **10**, 367 (2004).
- [11] E. Andjel and R. B. Schinazi, *J. Appl. Prob.* **33**, 741 (1996).
- [12] K. Sato, H. Matsuda and A. Sasaki, *J. Math. Bio.* **32**, 251 (1994).
- [13] K. Tainaka, *Phys. Lett. A* **176**, 303 (1993)
- [14] K. Tainaka, *J. Theor. Biol.* **166**, 91 (1994).
- [15] M. Peltomäki, V. Vuorinen, M. Alava and M. Rost, arXiv:cond-mat/0501743
- [16] K. Sato, N. Yoshida and N. Konno, *Appl. Math. Comp.* **126**, 255 (2002).
- [17] N. Konno, *Phase Transitions of Interacting Particle Systems* (World Scientific, Singapore, 1994).

FIGURE CAPTIONS

FIG. 1 (a)The rules of state transition of the SSE model. Dashed lines show transition probabilities proportional to the number of neighbors. Solid lines represent constant transition probabilities. (b)Rough sketch of the combination of the rules.

FIG. 2 Phase diagrams for (a) $\delta = 0$ and (b) $\delta = 1$ obtained by the MFA (solid lines), the PA (dashed lines), and MC simulations (solid circles).

FIG. 3 Dependence of $\rho(1)$ (MFA: thin solid lines, PA: thick solid lines, MC: triangles) and $\rho(2)$ (MFA: thin dotted lines, PA: thick dotted lines, MC: circles) on λ when (a) $(\mu, \delta)=(1,0)$ and (b) $(\mu, \delta)=(1,1)$.

FIG. 4 Dependence of $\rho(1)$ and $\rho(2)$ on μ when (a) $(\lambda, \delta)=(1,0)$ and (b) $(\lambda, \delta)=(1,1)$. See the caption of Fig. 2 for legends.

FIG. 5 The values of $\rho(ii)/\rho(i)^2$ for the PA with $\delta = 0$ (dotted lines) and $\delta = 1$ (dot-dashed-lines), compared with MC simulations with $\delta = 0$ (closed circles) and with $\delta = 1$ (open circles). We set $\mu = 1$ in (a, b, c) and $\lambda = 1$ in (d, e, f). Vertical lines represent critical points obtained by Eq. (26).

FIG. 6 The values of $\rho(ij)/[\rho(i)\rho(j)]$ for the PA with $\delta = 0$ and $\delta = 1$, compared with MC results. We set $\mu = 1$ in (a, b, c) and $\lambda = 1$ in (d, e, f). See the caption of Fig. 4 for legends.

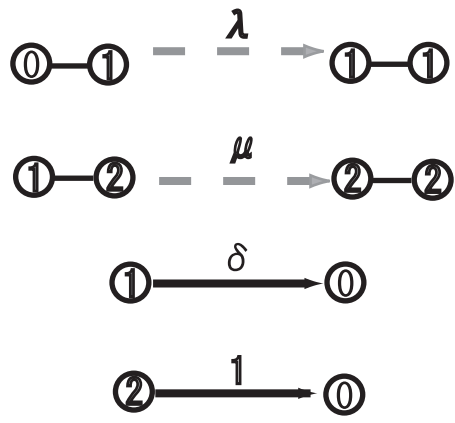


FIG. 1 Ohtsuka et al.

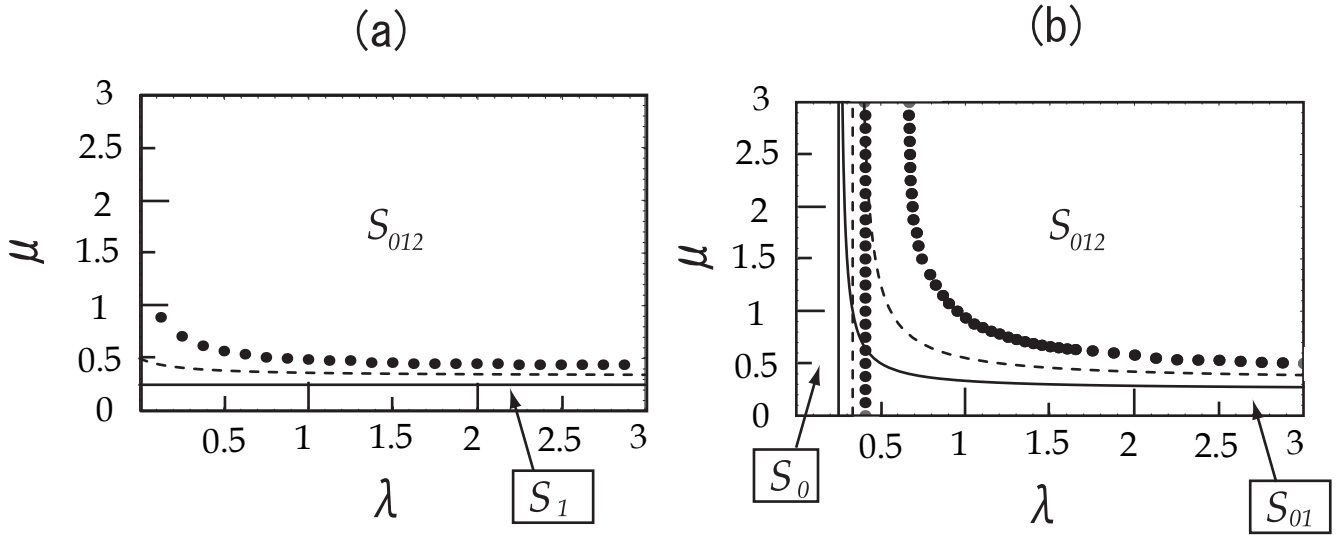


FIG. 2 Ohtsuka et al.

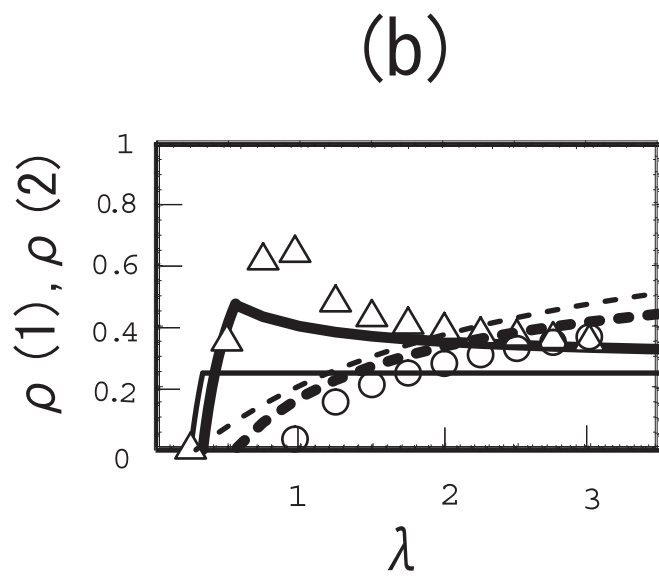
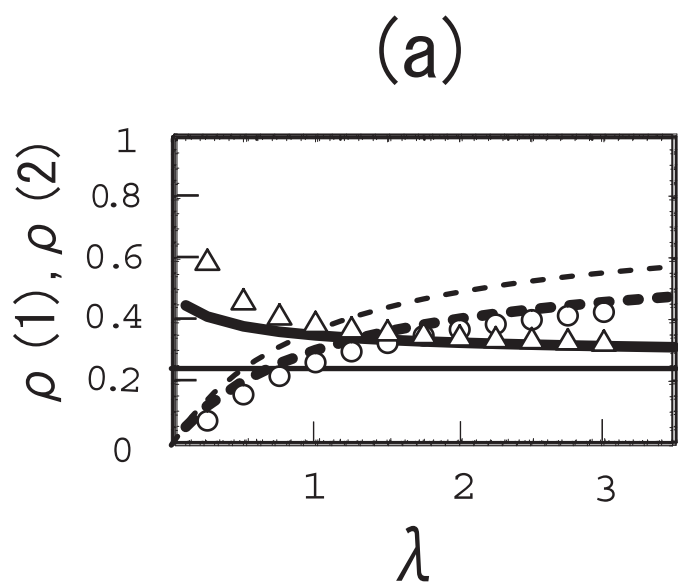
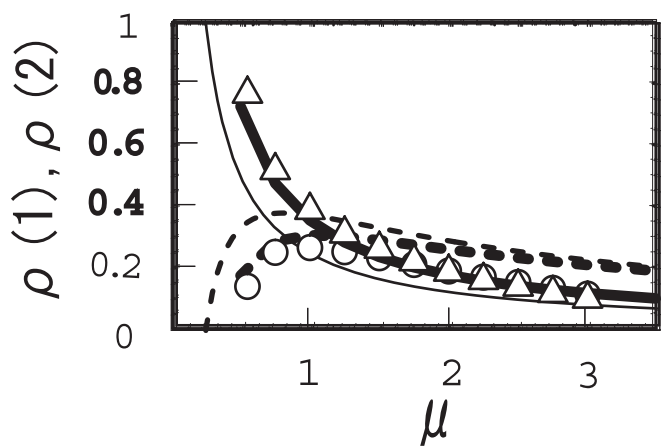


FIG. 3 Ohtsuka et al.

(a)



(b)

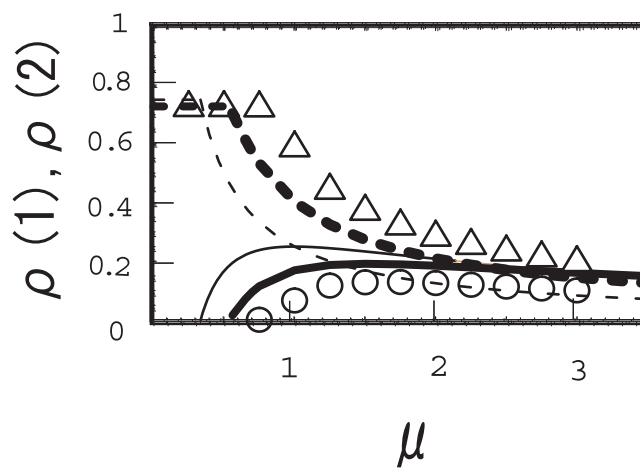


FIG. 4 Ohtsuka et al.

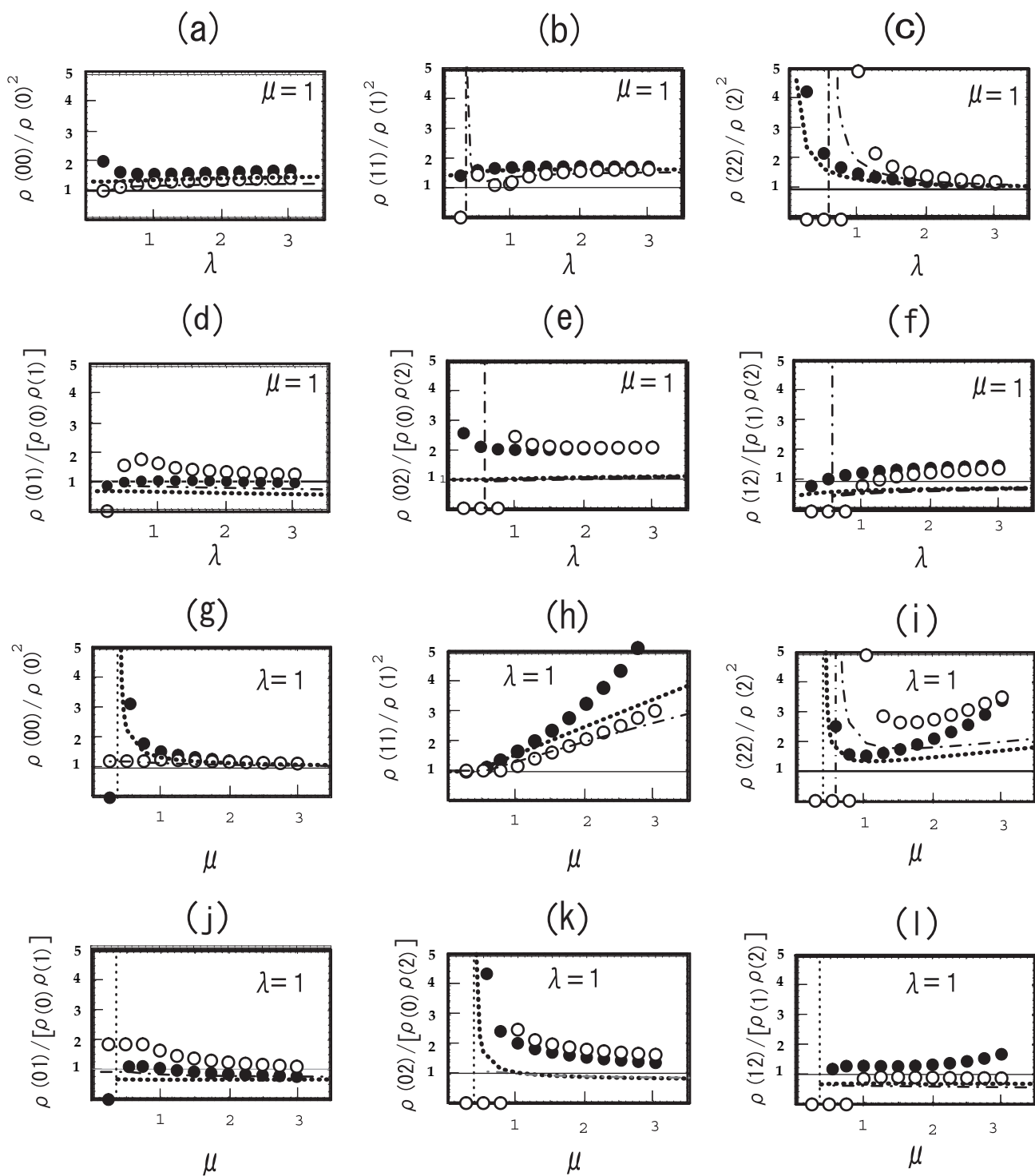


FIG. 5 Ohtsuka et al.